



# Institutional Repository - Research Portal

## Dépôt Institutionnel - Portail de la Recherche

researchportal.unamur.be

## RESEARCH OUTPUTS / RÉSULTATS DE RECHERCHE

### **Influence of nitrogen on the growth and luminescence of silicon nanocrystals embedded in silica**

Bolduc, M.; Genard, G.; Yedji, M.; Barba, D.; Martin, F.; Terwagne, G.; Ross, G.G.

*Published in:*  
Journal of Applied Physics

*DOI:*  
[10.1063/1.3054561](https://doi.org/10.1063/1.3054561)

*Publication date:*  
2009

*Document Version*  
Early version, also known as pre-print

[Link to publication](#)

*Citation for published version (HARVARD):*  
Bolduc, M, Genard, G, Yedji, M, Barba, D, Martin, F, Terwagne, G & Ross, GG 2009, 'Influence of nitrogen on the growth and luminescence of silicon nanocrystals embedded in silica' Journal of Applied Physics, vol. 105, no. 1. <https://doi.org/10.1063/1.3054561>

#### **General rights**

Copyright and moral rights for the publications made accessible in the public portal are retained by the authors and/or other copyright owners and it is a condition of accessing publications that users recognise and abide by the legal requirements associated with these rights.

- Users may download and print one copy of any publication from the public portal for the purpose of private study or research.
- You may not further distribute the material or use it for any profit-making activity or commercial gain
- You may freely distribute the URL identifying the publication in the public portal ?

#### **Take down policy**

If you believe that this document breaches copyright please contact us providing details, and we will remove access to the work immediately and investigate your claim.

## Influence of nitrogen on the growth and luminescence of silicon nanocrystals embedded in silica

M. Bolduc,<sup>1</sup> G. Genard,<sup>2</sup> M. Yedji,<sup>1</sup> D. Barba,<sup>1</sup> F. Martin,<sup>1</sup> G. Terwagne,<sup>2</sup> and G. G. Ross<sup>1,a)</sup>

<sup>1</sup>*INRS-Énergie, Matériaux et Télécommunications, 1650, Blvd. Lionel-Boulet, Varennes, Québec J3X 1S2, Canada*

<sup>2</sup>*Centre de Recherche en Physique de la Matière et du Rayonnement, Laboratoire d'Analyses par Réactions Nucléaires, University of Namur (FUNDP), 61 Rue de Bruxelles, B-5000 Namur, Belgium*

(Received 6 June 2008; accepted 12 November 2008; published online 9 January 2009)

Silicon nanocrystals (Si-ncs) have been produced by implantation of Si<sup>+</sup> in excess into SiO<sub>2</sub> followed by both annealing and passivation using argon or nitrogen. Nitrogen increases the photoluminescence (PL) emission and shifts the spectra toward the blue. The measured Si-nc diameter is 4.3 and 3.8 nm after annealing performed under Ar and N<sub>2</sub>, respectively. A significant quantity of nitrogen atoms has been detected in all samples by resonant nuclear reaction analysis (RNRA). The nitrogen concentration is significantly higher when the annealing and passivation are performed in a nitrogen environment, in agreement with a larger Si–N vibration signal on the Raman spectra. The depth profiles of nitrogen are very similar to those of Si-nc, suggesting that the N<sub>2</sub> molecules may diffuse in the SiO<sub>2</sub> during the annealing and then are trapped in proximity to the Si-nc. In addition to Si<sup>+</sup>, the implantation of N<sub>2</sub><sup>+</sup> to concentrations of 3 and 6 at. % produced a decrease in the PL intensity (accentuated at the higher concentration) and an increase in the Raman signal associated to Si–N vibrations. These results suggest that a relatively low nitrogen atomic fraction enhances the PL emission, since a large nitrogen concentration impedes the formation of Si-nc thus significantly decreasing the PL intensity. © 2009 American Institute of Physics.

[DOI: [10.1063/1.3054561](https://doi.org/10.1063/1.3054561)]

### I. INTRODUCTION

Since the discovery by Canham<sup>1</sup> in 1990 showing that Si nanostructures can emit light at room temperature, there has been a considerable amount of interest on Si nanoclusters.<sup>2,3</sup> Silicon nanometer-sized particles present unique optical properties, which are not observed in bulk materials. In particular, once excited by photons, silicon nanocrystals (Si-nc) exhibit strong visible luminescence even at room temperature. The Si-nc can be easily produced either by deposition of substoichiometric SiO<sub>2</sub> layer or by ion implantation of excess silicon in silicon oxide amorphous materials, followed by thermal annealing in an inert atmosphere.<sup>4–8</sup> The light emission of Si-nc was attributed by some authors to a quantum confinement effect, but it is now considered that this model cannot explain all the reported experimental data<sup>9</sup> and that the nature and the optical properties of the SiO<sub>2</sub> where the Si-nc are formed can strongly affect the photoluminescence (PL) spectra.<sup>10</sup> The physicochemical composition of the SiO<sub>2</sub> layer surrounding the Si-nc plays an important role in light emission and in optical gain. For example, the growth of substoichiometric SiO<sub>2</sub> deposited layer is different when N<sub>2</sub>O or O<sub>2</sub>, used as an oxidizing precursor gas, is mixed with the usual SiH<sub>4</sub> gas. Muloni *et al.*<sup>11</sup> performed physicochemical characterization of the deposited layers before and after annealing at different temperatures. They investigated the possible role of nitrogen in the Si-nc formation. Using secondary ion mass spectrometry (SIMS), a large

quantity of nitrogen (~15%) in the layer deposited with a SiH<sub>4</sub>–N<sub>2</sub>O gas mixture has been found even after annealing at 1200 °C. In this case, only a small nitrogen fraction was replaced at the surface by oxidizing oxygen. On the other hand, a smaller, but significant, quantity of nitrogen (~2%–3%) was detected in the layer deposited with a SiH<sub>4</sub>–O<sub>2</sub> gas mixture only after annealing. X-ray photoelectron spectroscopy (XPS) revealed that a larger concentration of Si–Si bonds is observed after annealing in the sample deposited with the O<sub>2</sub> oxidizing precursor gas. According to these authors, it seems that the presence of nitrogen inhibits the Si diffusion, thus influencing the Si-nc growth rate.

More recently, Wilkinson and Elliman<sup>12</sup> reported that the shape and intensity of the PL spectra emitted from Si-nc produced by ion implantation is strongly influenced by the choice of the annealing environment (Ar, N<sub>2</sub>, or 5% H<sub>2</sub> in N<sub>2</sub>). Samples annealed in Ar exhibit a less intense redshifted PL spectrum. Raman spectroscopy measurements indicate that the annealing in N<sub>2</sub> gas reduces the Si-nc mean size due to the possible formation of a very thin oxinitride layer at the Si-nc/SiO<sub>2</sub> interface. These authors concluded that these results are consistent with the fact that the annealing in Ar or N<sub>2</sub> is a process of thermal relaxation. However, in the case of N<sub>2</sub>, the compound formation arises through the diffusion of ambient nitrogen into the oxide matrix. Unfortunately, there were no direct measurements of the nitrogen content in these Si-nc/SiO<sub>2</sub> samples and no indication on a possible role of nitrogen on the growth of Si-nc. Moreover, no value of the Si-nc diameter and size distribution was determined. The aim of this paper is to present evidence that a given quantity of nitrogen atoms is incorporated into the Si-nc/SiO<sub>2</sub> layer and

<sup>a)</sup>Author to whom correspondence should be addressed. Tel.: +1 450-929-8108. Electronic mail: [ross@emt.inrs.ca](mailto:ross@emt.inrs.ca).

that the nitrogen concentration has a direct influence on the growth of the Si-nc, strongly affecting the PL spectra.

## II. EXPERIMENTAL

Two different types of samples were used in our study: amorphous fused silica and films ( $\sim 1 \mu\text{m}$ ) of amorphous  $\text{SiO}_2$  thermally grown on a Si (100) substrate.<sup>13</sup> The former samples are to verify that the PL spectra are not influenced by interference phenomena<sup>14,15</sup> while the latter samples facilitate characterization using nuclear reaction by avoiding the accumulation of electric charges during irradiation.<sup>16,17</sup> Quartz and  $\text{SiO}_2$  samples were implanted by means of the IMC-200 ion implanter<sup>18</sup> with 150 keV  $\text{Si}^+$  ions to a fluence of  $1.1 \times 10^{17} \text{ Si}^+/\text{cm}^2$ , which corresponds to local Si concentration in excess of 23 at. % at the mean implantation depth ( $R_p$ ). All samples were implanted simultaneously with fluence uniformity better than 1%. After the  $\text{Si}^+$  implantation, some samples were also implanted with 164 keV  $\text{N}_2^+$  ions to fluences of  $3 \times 10^{16}$  and  $6 \times 10^{16} \text{ N/cm}^2$ . According to SRIM simulation,<sup>19</sup> this energy produces an implantation mean range very similar to that of the excess Si. Thereafter, the samples were annealed to 1100 °C for 60 min under an environment of nitrogen ( $\text{N}_2$ ) or argon (Ar). Some samples were passivated at 500 °C for 30 min in a forming gas of 5%  $\text{H}_2$ +95%  $\text{N}_2$  or 5%  $\text{H}_2$ +95% Ar. Measurements of the photoluminescence (PL) were carried out at ambient temperature using a laser diode at 405 nm for photonic excitation. The light emitted by the sample was transmitted to an optical-multichannel spectrometer (Ocean Optics USB2000). The wavelength detection of the spectroscopy extends between 550 and 1100 nm.

Micro-Raman measurements were performed at room temperature using a confocal Invia Renishaw RM 3000 spectrometer, equipped with a digital camera and a 50 $\times$  objective lens of 0.75 numerical aperture (NA). An Ar laser line at 514.5 nm, focused either on the sample surface or within the first micrometer of the sample, was used for the Raman excitation.<sup>20</sup>

The nitrogen profiles were measured by resonant nuclear reaction analysis (RNRA) using the  $^{14}\text{N}(\alpha, \gamma)^{18}\text{F}$  nuclear reaction, which has a resonance at 1.531 MeV.<sup>21</sup> The advantage of RNRA is the narrow resonance exhibited by the cross section leading to an excellent depth resolution of the nitrogen profiles.<sup>22–24</sup> The reported values for the  $^{14}\text{N}(\alpha, \gamma)^{18}\text{F}$  resonance are: width of 0.6 keV<sup>21</sup> and resonance strength of 2.6 eV.<sup>25</sup> From these values, a resonant cross section of 3.1 mb was calculated.<sup>26</sup> All RNRA measurements were done with the ALTAIS,<sup>27</sup> the linear accelerator installed at LARN. The experimental setup is described in more details elsewhere.<sup>22</sup> The  $^{14}\text{N}$  depth profiles are measured by varying step by step the incident  $^4\text{He}^+$  energy, so that the resonant cross section acts as a probe of the nitrogen depth distribution. At each energy, gamma rays in the range of 3.06–5.60 MeV produced by de-excitation of the  $^{18}\text{F}$  nuclei were counted in a NaI(Tl) well detector.

In order to measure the nitrogen concentration with greater sensitivity than the resonant reaction  $^{14}\text{N}(\alpha, \gamma)^{18}\text{F}$ , the  $^{14}\text{N}(d, \alpha)^{12}\text{C}$  and  $^{14}\text{N}(d, p)^{15}\text{N}$  nuclear reactions were

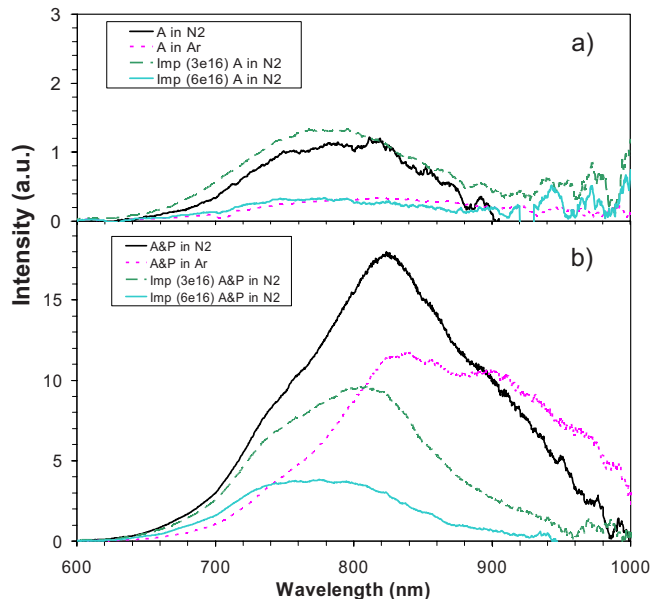


FIG. 1. (Color online) PL spectra of samples (a) annealed and (b) annealed and passivated under  $\text{N}_2$  or Ar environment. Two samples were also implanted with different nitrogen fluences ( $3 \times 10^{16}$  and  $6 \times 10^{16} \text{ N/cm}^2$ ) before annealing.

used with 1.05 MeV deuterons particles. The detector used for nuclear reaction analysis (NRA) was placed at 150° relatively to the incident beam direction and a 12  $\mu\text{m}$  Mylar absorber was placed in front of the detector to stop deuterons backscattered on the target. A rectangular 4  $\times$  13  $\text{mm}^2$  collimator placed in front of the detector defines a solid angle of 20.8 msr. Another detector used for Rutherford backscattering spectroscopy (RBS) was placed at 165° relatively to the incident beam direction in order to measure the number of incident particles. The sensitivity of  $^{14}\text{N}(d, \alpha)^{12}\text{C}$  and  $^{14}\text{N}(d, p)^{15}\text{N}$  reactions is typically of  $\sim 10^{15} \text{ atoms/cm}^2$ .

## III. RESULTS AND DISCUSSION

The PL spectra of annealed and annealed/passivated samples are shown in Figs. 1(a) and 1(b), respectively. It is obvious that the passivation procedure and the type of annealing gas used have a strong influence on both the intensity and the shape of the PL spectra. Annealing in  $\text{N}_2$  promotes an increase in the PL intensity along with a blueshift of the spectra in comparison to samples annealed in Ar [Fig. 1(a)]. After passivation, the difference in intensity between the samples annealed in Ar and in  $\text{N}_2$  is relatively smaller [Fig. 1(b)] and the spectrum of the  $\text{N}_2$  treated sample is significantly blueshifted in comparison to the Ar treated sample, in agreement with the observation of Wilkinson and Elliman.<sup>12</sup>

Nitrogen implantation also has a strong influence on the PL. It produces a blueshift that is accentuated by passivation. For the passivated samples [Fig. 1(b)], the PL intensity is lower for those that have been implanted, notably at the higher nitrogen fluence ( $6 \times 10^{16} \text{ N/cm}^2$ ). In contrast, for annealed only samples [Fig. 1(a)], the PL intensity is greatest for the sample implanted with the lower nitrogen fluence ( $3 \times 10^{16} \text{ N/cm}^2$ ). This result supports the hypothesis that the presence of nitrogen contributes to passivate the dangling

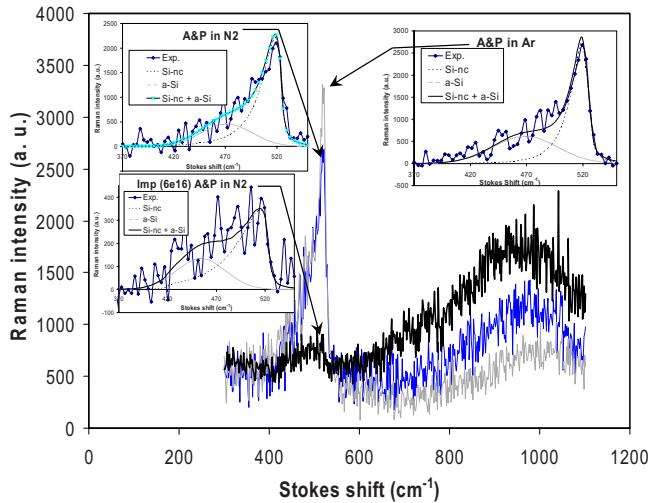


FIG. 2. (Color online) Raman spectra of samples annealed and passivated in  $N_2$  or in Ar environment. One sample was also implanted with nitrogen before annealing. The inset shows a detail view of the peak at  $520\text{ cm}^{-1}$  and the result of the fit for the  $I_{\alpha\text{-Si}}$  at  $470\text{ cm}^{-1}$  and  $I_{\text{Si-nc}}$  at  $520\text{ cm}^{-1}$ .

bonds, promoting radiative transitions. However, it seems that a too large nitrogen concentration leads to an attenuation of the PL emission.

In order to clarify this observation, the annealed/passivated samples have been characterized by Raman spectroscopy and the results are shown in Fig. 2. The sharp peak around  $520\text{ cm}^{-1}$  is the optical phonon associated with Si-nc.<sup>28–32</sup> The intensity and shape of this peak is influenced by the size and concentration of Si-nc. The peak intensity is slightly higher for the sample annealed under Ar, suggesting that the Si-nc size could be larger. This is in agreement with the observed redshift of the PL spectra in Fig. 1. However, the most remarkable result is the low Raman signal observed in the nitrogen implanted sample. This suggests that the high nitrogen concentration reduces the formation of Si-nc, which may explain the weak PL signal recorded from this sample.

From Raman characterization, it is possible to obtain information about the Si-nc size and the ratio of the Si amorphous clusters ( $\alpha\text{-Si}$ ) phonon peak intensity ( $I_{\alpha\text{-Si}}$ ), around  $470\text{ cm}^{-1}$ , to the Si-nc optical vibration modes ( $I_{\text{Si-nc}}$ ), around  $520\text{ cm}^{-1}$ .<sup>20</sup> An instrumental resolution of  $5\text{ cm}^{-1}$  and a reference wave number of  $524\text{ cm}^{-1}$  for the Si-Si bond in bulk  $^{28}\text{Si}$  were used to fit the experimental results to obtain the Si-nc diameter and size distribution. We use a reference wave number of  $524\text{ cm}^{-1}$  for the Si-Si bond because the Si-nc nucleation comes from the clustering of implanted Si and our ion implantations were performed with  $^{28}\text{Si}$  (i.e., not with natural Si).<sup>33</sup> The fit is plotted in the inset

TABLE I. Si-nc diameter and size distribution and  $I_{\alpha\text{-Si}}/I_{\text{Si-nc}}$  ratio for different samples.

Sample	Si-nc diameter	Si-nc size distribution	$I_{\alpha\text{-Si}}/I_{\text{Si-nc}}$
A and P in Ar	$4.3(\pm 0.1)\text{ nm}$	$0.7(\pm 0.1)\text{ nm}$	$22.2(\pm 5)\%$
A and P in $N_2$	$3.8(\pm 0.1)\text{ nm}$	$0.7(\pm 0.1)\text{ nm}$	$21.5(\pm 5)\%$
Imp. ( $6 \times 10^{16}\text{ N/cm}^2$ )	$3.0(\pm 0.3)\text{ nm}$	$0.5(\pm 0.3)\text{ nm}$	$35.0(\pm 15)\%$

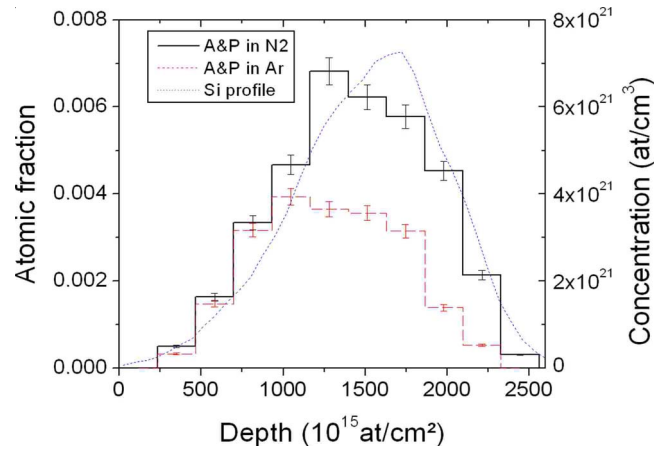


FIG. 3. (Color online) RNRA depth profile of nitrogen in samples annealed and passivated under  $N_2$  or Ar environment, along with the Si depth profile simulated with the SRIM software.

of Fig. 2 and the results are presented in Table I. These indicate that the use of a  $N_2$  environment produces smaller Si-nc than annealing under Ar, in agreement with Wilkinson and Elliman.<sup>12</sup> The choice of the annealing gas (Ar or  $N_2$ ) has no influence on the Si-nc size distribution or on the  $I_{\alpha\text{-Si}}/I_{\text{Si-nc}}$  ratio, suggesting that the presence of nitrogen does not contribute to the formation and crystallization of Si-nc. These observations are in contradiction with the conclusion of Muloni *et al.*<sup>11</sup> who used a different technique in the deposition of substoichiometric  $\text{SiO}_2$  layers. Finally,  $N_2^+$  ion-implanted samples show the smallest Si-nc diameter and the greatest  $I_{\alpha\text{-Si}}/I_{\text{Si-nc}}$  ratio. Although the differences in Si-nc size distribution and  $I_{\alpha\text{-Si}}/I_{\text{Si-nc}}$  ratio are less than the respective measurement error, nevertheless these measurements suggest that a high nitrogen concentration may lead to an occupation of one or more Si bonds, thus impeding the formation of Si-nc leaving the Si atoms in amorphous clusters. Thus, there is a strong possibility that the Si-nc concentration has been decreased by the implantation of nitrogen.

A peak is also observed around  $950\text{ cm}^{-1}$  in the Raman spectrum of Fig. 2. This peak is associated to the Si-N bond,<sup>34,35</sup> which can provide very useful information on the role of nitrogen in the PL. It is obvious that annealing/passivation in  $N_2$  environment has contributed to enhance the formation of Si-N bonds, supporting the hypothesis that nitrogen plays a passivation role during annealing. Another striking result is the high intensity of the Si-N peak observed in the nitrogen implanted sample. This supports the fact that nitrogen atoms in high concentration can occupy a larger number of Si bonds, preventing an efficient formation of Si-nc. This observation is in agreement with the results of Table I and the weakness of the Si-nc peak around  $500\text{ cm}^{-1}$ .

Depth profiles of nitrogen, as measured by the RNRA technique, are shown in Fig. 3 for samples annealed and passivated in Ar and  $N_2$ . A high nitrogen concentration is observed from the samples annealed and passivated in  $N_2$ . In both cases, the nitrogen depth profiles correspond to the Si depth profile also shown in Fig. 3. In order to distinguish between implanted and annealed nitrogen atoms, nonannealed control samples of nonimplanted and  $\text{Si}^+$  ion-

TABLE II. Areal nitrogen density as measured by NRA in different samples.

Sample description	Nitrogen areal concentration
Non implanted SiO <sub>2</sub>	$<1 \times 10^{15}$ N/cm <sup>2</sup>
Si implanted SiO <sub>2</sub> (not annealed)	$3.4 \times 10^{15}$ N/cm <sup>2</sup>
Si implanted SiO <sub>2</sub> (A in Ar)	$4.1 \times 10^{15}$ N/cm <sup>2</sup>
Si implanted SiO <sub>2</sub> (A and P in Ar)	$8.2 \times 10^{15}$ N/cm <sup>2</sup>
Si implanted SiO <sub>2</sub> (A in N <sub>2</sub> )	$1.0 \times 10^{16}$ N/cm <sup>2</sup>
Si implanted SiO <sub>2</sub> (A and P in N <sub>2</sub> )	$1.4 \times 10^{16}$ N/cm <sup>2</sup>

implanted samples have been fabricated for NRA characterization since both Si atoms and N<sub>2</sub> molecules have mass of 28 and follow similar trajectory in the magnetic field of the ion implanter. The areal concentrations of nitrogen are shown in Table II along with those measured in annealed and annealed/passivated samples. The sensitivity of the characterization technique ( $\sim 1 \times 10^{15}$  at/cm<sup>2</sup>) has been determined from nonimplanted control samples. However, a very small quantity of nitrogen was detected in the implanted sample, indicating that some N<sub>2</sub><sup>+</sup> ions were implanted during the Si<sup>+</sup> implantation. Annealing and passivation in Ar have not significantly increased the nitrogen concentration, while a slightly higher quantity of nitrogen was detected in the sample passivated at 500 °C. On the other hand, annealing and passivation in N<sub>2</sub> environment have significantly increased the nitrogen concentration. These measurements support the hypothesis that a small quantity of nitrogen can diffuse in the sample during both annealing and passivation. Since the nitrogen depth profiles follow that of the implanted Si, the diffused nitrogen can be trapped in the region where excess Si is localized. This is strengthened by the observation of Si–N bonds through Raman spectroscopy.

It is well known that N<sub>2</sub> can diffuse into SiO<sub>2</sub> at high temperature  $\sim 1100$  °C (Ref. 36) and can be incorporated at the Si/SiO<sub>2</sub> interface as an oxynitride compound.<sup>12,35,37</sup> The implantation induced damage can also contribute to enhance the N<sub>2</sub> diffusion. According to the Raman and nuclear (RNRA and NRA) characterizations, the N<sub>2</sub> diffused throughout the SiO<sub>2</sub> films and was trapped at the Si-nc/SiO<sub>2</sub> interface. The similarity of the nitrogen and Si-nc depth profiles, combined to the observation of an increase in the Si–N bonds in samples annealed in N<sub>2</sub> environment, support the mechanism proposed by Wilkinson and Elliman<sup>12</sup> that annealing in N<sub>2</sub> is a process of thermal relaxation that is compounded by the exchange of nitrogen with the oxide network. The blueshift of the PL spectra could be a consequence of the size reduction in the Si-nc by oxynitridation at the Si-nc/SiO<sub>2</sub> interface. The observation of Si–N bond vibrations suggests the formation of SiO<sub>x</sub>N<sub>y</sub> compounds in similitude with the mechanism observed at the Si/SiO<sub>2</sub> interface during annealing in nitrogen.<sup>36</sup> At low concentration, the presence of nitrogen can contribute to the passivation of the Si-nc/SiO<sub>2</sub> interface in reducing the number of point defects or isolated dangling bonds<sup>38</sup> due to a better molecular matching at the Si/SiO<sub>x</sub>N<sub>y</sub> interface (in comparison to the Si/SiO<sub>2</sub> interface).<sup>39</sup> Consequently, the PL intensity increases as has been observed after hydrogen passivation. However, at high

concentration, for instance when N<sub>2</sub> ions were implanted, the oxynitridation is not stopped by lack of N<sub>2</sub>, thus the Si-nc size is strongly reduced and may eventually not be formed. This mechanism is supported by the results in Table I, concerning the Si-nc size and the  $I_{\alpha\text{-Si}}/I_{\text{Si-nc}}$  ratio.

#### IV. CONCLUSION

PL emission of Si-nc produced by implantation of Si<sup>+</sup> in excess into SiO<sub>2</sub> is increased when a nitrogen environment is used during annealing. A blueshift in the PL spectra has been observed in agreement with the decrease in the Si-nc diameter from 4.3 to 3.8 nm when Ar and N<sub>2</sub> gases are used, respectively. Nitrogen atoms have been detected in all samples by RNRA and the nitrogen concentration is significantly higher when the annealing and passivation are performed under N<sub>2</sub> environment. The nitrogen depth-profiles are closely related to those of Si-nc, suggesting that the nitrogen atoms diffuse in the SiO<sub>2</sub> during the annealing and can be trapped in proximity of the Si-nc. This hypothesis is supported by the observation of a higher Si–N bond concentration through Raman spectroscopy. The implantation of nitrogen to nitrogen concentrations of 3 and 6 at. % has decreased the PL intensity. These results suggest that a relatively low atomic fraction of nitrogen has enhanced the PL emission while at high nitrogen concentration, the formation of Si-nc is reduced, leading to a decrease in the PL intensity.

#### ACKNOWLEDGMENTS

The authors thank Gilles Abel for technical help and ion implantation processing. This work has been supported by the ST-4/05.804 collaboration between the Wallonie-Bruxelles Community and the government of Québec, and the Natural Science and Engineering Research Council of Canada (NSERC, Grant No. STPSC 356653-07). G. Genard was supported as research fellow by the Belgian National Fund for Scientific Research (F.R.S.-FNRS).

- <sup>1</sup>L. T. Canham, *Appl. Phys. Lett.* **57**, 1046 (1990); A. G. Cullis, L. T. Canham, and P. D. Calcott, *J. Appl. Phys.* **82**, 909 (1997).
- <sup>2</sup>D. J. DiMaria, J. R. Kirtley, E. J. Pakulis, D. W. Dong, T. S. Kuan, F. L. Pesavento, T. N. Theis, and J. A. Cutro, *J. Appl. Phys.* **56**, 401 (1984).
- <sup>3</sup>S. Hayashi, T. Nagareda, Y. Kanzawa, and K. Yamamoto, *Jpn. J. Appl. Phys., Part 1* **32**, 3840 (1993).
- <sup>4</sup>S. Cheylan, N. B. Manson, and R.G. Elliman, *J. Lumin.* **80**, 213 (1998).
- <sup>5</sup>S. Cheylan and R.G. Elliman, *Nucl. Instrum. Methods Phys. Res. B* **148**, 986 (1999).
- <sup>6</sup>T. Shimizu-Iwayama, K. Fujita, S. Nakao, K. Saitoh, T. Fujita, and N. Itoh, *J. Appl. Phys.* **75**, 7779 (1994).
- <sup>7</sup>T. Komoda, J. P. Kelly, R. M. Gwilliam, P. L. F. Hemment, and B. J. Sealy, *Nucl. Instrum. Methods Phys. Res. B* **112**, 219 (1996).
- <sup>8</sup>B. Garrido, M. López, S. Ferré, A. Romano-Rodríguez, A. Pérez-Rodríguez, P. Ruterana, and J. R. Morante, *Nucl. Instrum. Methods Phys. Res. B* **120**, 101 (1996).
- <sup>9</sup>F. Koch and V. Petrova-Koch, *J. Non-Cryst. Solids* **198–200**, 840 (1996).
- <sup>10</sup>S. M. Orbons, M. G. Spooner, and R. G. Elliman, *J. Appl. Phys.* **96**, 4650 (2004).
- <sup>11</sup>V. Mulloni, P. Bellutti, and L. Vanzetti, *Surf. Sci.* **585**, 137 (2005).
- <sup>12</sup>A. R. Wilkinson and R. G. Elliman, *J. Appl. Phys.* **96**, 4018 (2004).
- <sup>13</sup>Supplied by Universitywafer.com, 66 N Street, Unit #9, South Boston, MA 02127.
- <sup>14</sup>R. Smirani, F. Martin, G. Abel, Y. Q. Wang, M. Chicoine, and G. G. Ross, *J. Lumin.* **115**, 62 (2005).

- <sup>15</sup>D. Barba, F. Martin, C. Dahmoune, and G. G. Ross, *Appl. Phys. Lett.* **89**, 034107 (2006).
- <sup>16</sup>G. G. Ross and C. Sévigny, *Nucl. Instrum. Methods Phys. Res. B* **211**, 351 (2003).
- <sup>17</sup>M. Yedji and G. G. Ross, *J. Phys. D* **39**, 4429 (2006).
- <sup>18</sup>Purchased from Ion Beam Services: <http://www.ion-beam-services.com/>.
- <sup>19</sup>J. P. Biersack and J. F. Ziegler, SRIM-2006; <http://www.srim.org>.
- <sup>20</sup>D. Barba, F. Martin, and G. G. Ross, *Nanotechnology* **19**, 115707 (2008).
- <sup>21</sup>C. R. Gossett, *Nucl. Instrum. Methods Phys. Res. B* **10–11**, 722 (1985).
- <sup>22</sup>G. Genard, M. Yedji, G. G. Ross, and G. Terwagne, *Nucl. Instrum. Methods Phys. Res. B* **264**, 156 (2007).
- <sup>23</sup>G. Terwagne, M. Piette, and F. Bodart, *Nucl. Instrum. Methods Phys. Res. B* **19–20**, 145 (1987).
- <sup>24</sup>G. Terwagne, S. Lucas, and F. Bodart, *Nucl. Instrum. Methods Phys. Res. B* **66**, 262 (1992).
- <sup>25</sup>H. B. Mak, G. T. Ewan, J. D. MacArthur, W. McLatchie, and R. E. Azuma, *Nucl. Phys. A* **343**, 79 (1980).
- <sup>26</sup>M. Yedji, M. Bolduc, G. Genard, G. Terwagne, and G. G. Ross, *Nucl. Instrum. Methods Phys. Res. B* **266**, 2060 (2008).
- <sup>27</sup>Accélérateur Linéaire Tandetron pour l'Analyse et l'Implantation des Solides.
- <sup>28</sup>G. H. Li, K. Ding, Y. Chen, H. X. Han, and Z. P. Wang, *J. Appl. Phys.* **88**, 1439 (2000).
- <sup>29</sup>H. Richter, Z. P. Wang, and L. Ley, *Solid State Commun.* **39**, 625 (1981).
- <sup>30</sup>I. H. Campbell and P. M. Fauchet, *Solid State Commun.* **58**, 739 (1986).
- <sup>31</sup>G. Faraci, S. Gibilisco, P. Russo, A. R. Pennisi, and S. La Rosa, *Phys. Rev. B* **73**, 033307 (2006).
- <sup>32</sup>Md. N. Islam, A. Pradhan, and S. Kumar, *J. Appl. Phys.* **98**, 024309 (2005).
- <sup>33</sup>M. Cardona, *Phys. Status Solidi B* **220**, 5 (2000).
- <sup>34</sup>B. K. Agrawal, P. S. Yadav, and B. K. Ghosh, *J. Phys. C* **21**, 3397 (1988).
- <sup>35</sup>M. Ribeiro, I. Pereyra, and M. I. Alayo, *Thin Solid Films* **426**, 200 (2003).
- <sup>36</sup>S. I. Raider, R. A. Gdula, and R. Petrak, *Appl. Phys. Lett.* **27**, 150 (1975).
- <sup>37</sup>M. L. Green, T. Sorsch, L. C. Feldman, W. N. Lennard, E. P. Gusev, E. Garfunkel, H. C. Lu, and T. Gustafsson, *Appl. Phys. Lett.* **71**, 2978 (1997).
- <sup>38</sup>B. Tuttle, *Phys. Rev. B* **60**, 2631 (1999).
- <sup>39</sup>E. P. Gusev, H. C. Lu, T. Gustafsson, E. Garfunkel, M. L. Green, and D. Brasen, *J. Appl. Phys.* **82**, 896 (1997).